Paper

FDTD Analysis of Effectiveness of Shielding Clothes in Suppressing Electromagnetic Field in Phantom Model

Yoshiyuki Yoshimura*,***, Student Member
Isamu Nagano*, Member
Satoshi Yagitani*, Non-member
Tomohiko Ueno*,***, Non-member
Toshihiro Nakayabu**, Non-member

Abstract In order to prevent cardiac pacemakers from malfunctioning caused by electromagnetic (EM) wave, as one of the solutions to the problem of pacemaker malfunctioning, we can use a shielding material to decrease the EM wave intensity. For the effective suppression of the EM wave including a complicated enclosure or a human body, it is desirable to solve for the EM wave propagation by using numerical analysis. We introduce the transmission coefficient when an EM wave is incident into a multi-layered material with an arbitrary direction into the FDTD method. This realizes three-dimensional numerical analysis of a thin shielding material as a method to solve the EM wave transmission problem, which has been conventionally considered difficult. We use a phantom model, a dummy model of a cardiac pacemaker wearer, to analyze the EM wave shielding effectiveness of the shielding clothes. The analytical result agrees fairly well with the experimental result, which verifies the validity of the developed method. As for the effect of the aperture of the shielding clothes, the EM wave coming around from the apertures is found to be larger in amount than the EM wave transmitted through the clothes, which suggests that the aperture causes the *SE* to decrease largely.

Keywords : electromagnetic shielding, FDTD, pacemaker, phantom, shielding clothes

1. Introduction

The rapid and remarkable progress in electronic information and communication technology has triggered the problem of malfunctioning of equipments caused by electromagnetic (EM) wave. For instance, the unwanted EM wave stops machines and the mobile phone causes cardiac pacemaker to malfunction. Particularly the explosive diffusion of mobile phones has become quite hazardous for the cardiac pacemaker users. Although it is recommended in Japan that the mobile phone users should keep a distance of 22 cm or more from the cardiac pacemaker users [1], there is no guarantee that the rule will be kept in crowded trains or department stores. Hence, the best way ensuring a substantial security would be to suppress the incoming EM wave with shielding materials. These shielding materials have conventionally been evaluated as simple plane materials so far. However, it is necessary to evaluate the performance when used as the enclosures and the clothes. Further, since the EM wave is diffracted from apertures on the shielding materials, the shielding effectiveness (*SE*) becomes different from the case of a simple plane material. Here, in order to shield the EM wave effectively, we have to investigate the EM wave propagation with the three-dimensional (3-D) object using the numerical analysis.

* Faculty of Engineering, Kanazawa University
2-40-20, Kodatsuno Kanazawa 920-8667
** Product and Technology Dep., Indust. Res. Inst. of Ishikawa
2-1, Kuratsuki, Kanazawa 920-8203
*** PFU Limited
Nu98-2, Unoke, Unoke-machi, Kahoku-gun, Ishikawa 929-1192

There are several methods of a numerical analysis. For instance, finite difference time domain (FDTD) method, finite element method, moment methods, and so on. The FDTD method is most commonly used for understanding the EM wave propagation process. The FDTD analysis must divide the 3-D object into the spatial cells of 1/10 wavelength, so that in the case of EM wave transmission through a thin shielding material plate, the number of cells increases and the analysis becomes more difficult. For avoiding this problem, there is the sub-grid method [2] where only the shielding material region is divided into smaller cells. However, the cell size unavoidably increases in a model of high conductivity material, and even in that case the error exists because of the use of interpolation on boundary. Further, there is a sub-cell method where substantially smaller cells are used against the spatial cell. This does not much increase the number of cells. This method has been applied to the problem of transmission through the thin metallic film [3][4]. In this case, however, the error increases depending on the material thickness and frequency. Further, another case has been reported that the transmission problem is calculated by introducing the shielding material into FDTD method as an infinite thin resistive film [5][6]. In this case the material thickness exceeding the skin depth and oblique incidence cause the error to increase. In this paper we improve the method in reference (6), and then suggest a method that agrees well with the theoretical result for the *SE* of the shielding material thicker than the skin depth and for the problem caused by oblique incidence [7].

Here, we evaluate the effectiveness of shielding clothes to

suppress the electromagnetic interference with a cardiac pacemaker. Several studies investigating the FDTD analysis of phantom have been reported so far [8][9], few papers have dealt with the analysis of EM wave suppressing effect of shielding clothes [10]-[12]. However the exact *SE* of the clothes has not been included in these calculations. In this paper, we extend the method in reference (7) to 3-D problem to implement FDTD analysis for obtaining the *SE* of the clothes covering a phantom. Further, the validity of this method is also discussed with experimental measurements using the phantom.

2. Introduction of Thin EM Shielding Materials in FDTD Analysis

When dealing with an extremely thin shielding material as compared with the wavelength in FDTD analysis, it is possible to derive effective formulation by using the theoretical transmission coefficient T and surface resistance R_s of the shielding material [6][7]. Here, we extend it to the 3-D model, which has not been reported so far with the oblique incidence.

2.1 Derivation of Transmission Coefficient As shown in Fig.1, we can derive the electromagnetic field incident into a multi-layered material with an arbitrary direction by resolving the incident fields into TE and TM mode components, then obtaining the EM fields of each mode, and finally the total wave fields composed of both modes of the vector components [13]. The electric fields $\boldsymbol{E}^{\mathrm{I}}$ (with unity amplitude) of the incident wave in each direction are defined by equation (1). The electric fields $\boldsymbol{E}^{\mathrm{T}}$ of the transmitted wave can be obtained by equation (2). Here the constants C are given by equation (3).

$$\left.\begin{aligned} E^{\mathrm{I}}_{x'0} &= \sin\phi\cos\theta_0 e^{jk_0(x'\sin\theta_0 - z'\cos\theta_0)} \\ E^{\mathrm{I}}_{y'0} &= \cos\phi e^{jk_0(x'\sin\theta_0 - z'\cos\theta_0)} \\ E^{\mathrm{I}}_{z'0} &= \sin\phi\sin\theta_0 e^{jk_0(x'\sin\theta_0 - z'\cos\theta_0)} \end{aligned}\right\} \quad \cdots\cdots (1)$$

$$\left.\begin{aligned} E^{\mathrm{T}}_{x'\mathrm{N}} &= -\frac{1}{C_{\mathrm{TM11}}}\frac{\eta_{\mathrm{N}}}{\eta_0}\sin\phi\cos\theta_{\mathrm{N}} e^{jk_{\mathrm{N}}(x'\sin\theta_{\mathrm{N}} - z'\cos\theta_{\mathrm{N}})} \\ E^{\mathrm{T}}_{y'\mathrm{N}} &= -\frac{1}{C_{\mathrm{TE11}}}\frac{\eta_{\mathrm{N}}}{\eta_0}\cos\phi e^{jk_{\mathrm{N}}(x'\sin\theta_{\mathrm{N}} - z'\cos\theta_{\mathrm{N}})} \\ E^{\mathrm{T}}_{z'\mathrm{N}} &= -\frac{1}{C_{\mathrm{TM11}}}\frac{\eta_{\mathrm{N}}}{\eta_0}\sin\phi\sin\theta_{\mathrm{N}} e^{jk_{\mathrm{N}}(x'\sin\theta_{\mathrm{N}} - z'\cos\theta_{\mathrm{N}})} \end{aligned}\right\} \quad \cdots\cdots (2)$$

$$\begin{bmatrix} C_{\mathrm{TE11}}, & C_{\mathrm{TE12}}, \\ \mathrm{TM11} & \mathrm{TM12} \\ C_{\mathrm{TE21}}, & C_{\mathrm{TE22}}, \\ \mathrm{TM21} & \mathrm{TM22} \end{bmatrix}$$

$$= \prod_{i=0}^{N-1} \frac{1}{2p_{\mathrm{TE}_i,\ \mathrm{TM}_i}} \times \begin{bmatrix} (p_{\mathrm{TE}_i,\ \mathrm{TM}_i} + p_{\mathrm{TE}_{i+1},\ \mathrm{TM}_{i+1}})e^{-j(q_i - q_{i+1})z_i'} & (p_{\mathrm{TE}_i,\ \mathrm{TM}_i} + p_{\mathrm{TE}_{i+1},\ \mathrm{TM}_{i+1}})e^{-j(q_i + q_{i+1})z_i'} \\ (p_{\mathrm{TE}_i,\ \mathrm{TM}_i} + p_{\mathrm{TE}_{i+1},\ \mathrm{TM}_{i+1}})e^{j(q_i + q_{i+1})z_i'} & (p_{\mathrm{TE}_i,\ \mathrm{TM}_i} + p_{\mathrm{TE}_{i+1},\ \mathrm{TM}_{i+1}})e^{j(q_i - q_{i+1})z_i'} \end{bmatrix} \quad \cdots\cdots (3)$$

where, the subscripts TM and TE indicate the mode components, i represents the i th layer, and

$$P_{\mathrm{TE}_i} = \frac{1}{\eta_i}\cos\theta_i,\ P_{\mathrm{TM}_i} = \eta_i\cos\theta_i$$

$$q_i = k_i\cos\theta_i,\ \eta_i = \sqrt{\frac{\mu_i}{\varepsilon_i}}$$

where, k_i is wave number, ε_i is permittivity, μ_i is permeability, and η_i is impedance. Here, from Snell's law:

$$\cos\theta_i = \sqrt{1 - \left(\frac{k_0\sin\theta_0}{k_i}\right)^2}$$

Next, since the plane of incidence (x'-z' plane) in Fig.1 changes according to the propagation direction of EM wave, it is necessary to change to the basic x-y-z coordinates system as shown in Fig.2. Thus, the electromagnetic fields in the x-y plane are expressed by equations (4) and (5), respectively, and the theoretical transmission coefficients T_x and T_y of the components in the x-y plane can be obtained by equation (6).

$$\left.\begin{aligned} E^{\mathrm{I}}_{x0} &= E^{\mathrm{I}}_{x'0}\cos\psi_0 - E^{\mathrm{I}}_{y'0}\sin\psi_0 \\ E^{\mathrm{I}}_{y0} &= E^{\mathrm{I}}_{x'0}\sin\psi_0 + E^{\mathrm{I}}_{y'0}\cos\psi_0 \end{aligned}\right\} \quad \cdots\cdots (4)$$

$$\left.\begin{aligned} E^{\mathrm{T}}_{x\mathrm{N}} &= E^{\mathrm{T}}_{x'\mathrm{N}}\cos\psi_{\mathrm{N}} - E^{\mathrm{T}}_{y'\mathrm{N}}\sin\psi_{\mathrm{N}} \\ E^{\mathrm{T}}_{y\mathrm{N}} &= E^{\mathrm{T}}_{x'\mathrm{N}}\sin\psi_{\mathrm{N}} + E^{\mathrm{T}}_{y'\mathrm{N}}\cos\psi_{\mathrm{N}} \end{aligned}\right\} \quad \cdots\cdots (5)$$

where, $\psi_{\mathrm{N}} = \psi_0$.

$$T_{x,y} = \left|\frac{E^{\mathrm{T}}_{x,y\mathrm{N}}}{\mathrm{E}^{\mathrm{I}}_{x,y0}}\right| \quad \cdots\cdots (6)$$

2.2 Formulation of FDTD Method Assuming the shielding material on the x-y plane, the E on this shielding material can be expressed as the FDTD equation (7), where R_S [14] can be obtained from equation (8) using the T of the shielding

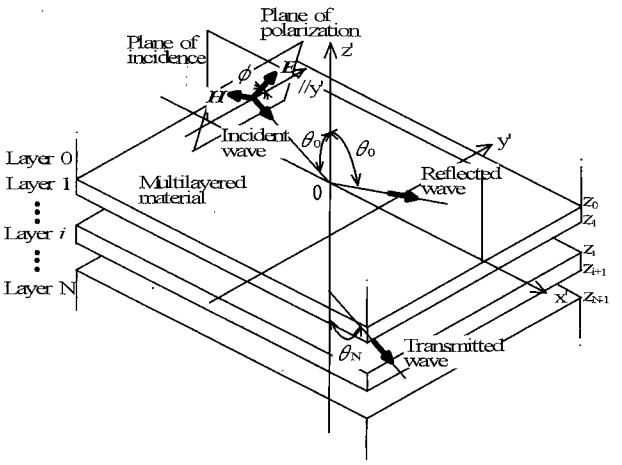

Fig. 1. Model of a multi-layered material with oblique incidence

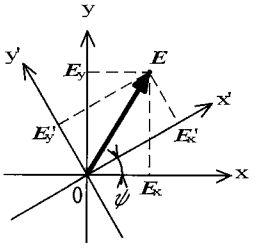

Fig. 2. Transformation of coordinates

material.

$$\left.\begin{aligned} E_x^n &= \frac{2\varepsilon\Delta z R_{Sx}-\Delta t}{2\varepsilon\Delta z R_{Sx}+\Delta t}E_x^{n-1}+\frac{2R_{Sx}\Delta z\Delta t}{2\varepsilon\Delta z R_{Sx}+\Delta t}\left(\frac{\Delta H_z^{n-\frac{1}{2}}}{\Delta y}-\frac{\Delta H_y^{n-\frac{1}{2}}}{\Delta z}\right)\\ E_y^n &= \frac{2\varepsilon\Delta z R_{Sy}-\Delta t}{2\varepsilon\Delta z R_{Sy}+\Delta t}E_y^{n-1}+\frac{2R_{Sy}\Delta z\Delta t}{2\varepsilon\Delta z R_{Sy}+\Delta t}\left(\frac{\Delta H_x^{n-\frac{1}{2}}}{\Delta z}-\frac{\Delta H_z^{n-\frac{1}{2}}}{\Delta x}\right)\end{aligned}\right\} \quad \cdots\cdots (7)$$

$$R_{Sx,y}=\frac{T_{x,y}\eta_0}{2-T_{x,y}-\frac{\eta_0}{\eta_N}T_{x,y}} \quad \cdots\cdots (8)$$

where, Δx, Δy and Δz are spatial grids, Δt is time increment, the superscript n is time step, and the subscripts x, y, and z indicate directions.

Where, in order to obtain T, ϕ and θ are derived by calculating Poynting vector incident onto each cell of the shielding material under the plane wave approximation. We implement similar calculation in a diffracted region. As for the magnetic fields $\boldsymbol{H}$, the original FDTD equation is used. Formulation is obtained similarly for the y-z plane and the z-x plane.

By arranging the above equations at the position of the shielding material, it is possible to analyze effectively the transmission of EM wave with an arbitrary incident direction.

2.3 Analysis Model and Calculation Conditions A box model (W:300×D:150×H:500 mm) is used as a phantom torso model. Further, the shielding clothes have apertures at the neck (W:160×D:150 mm) and waist (W:300×D:150 mm) regions. The shielding clothes are assumed as a single-layered material [15], with the material parameters assumed as shown in Table 1 [16][17] for comparing the calculated data with the experimental data. A wave of 900 MHz frequency from a half-wavelength dipole antenna [18] is used as the incident wave. The spatial cell is a cube (5×5×5 mm). Further, the scattered waves from the simulation space are absorbed by the 6-layered perfectly matched layer (PML) absorbing boundary conditions.

The *SE* can be obtained from equation (9) by the ratio of the electric field intensity ($\boldsymbol{E}_S$) with shielding clothes covering the phantom to that ($\boldsymbol{E}_0$) without the shielding clothes.

$$SE = 20\mathrm{Log}_{10}\frac{|\boldsymbol{E}_0|}{|\boldsymbol{E}_S|} \quad \cdots\cdots (9)$$

3. Phantom Experiment

As the phantom is used the acrylic container filled with the saline of 1.2 wt % NaCl with the electric parameters same as human in the experiment. The 900 MHz signal from the tracking generator (TG) of a spectrum analyzer (Advantest: R3361A) is radiated through a half-wave length dipole antenna (Schwarzbeck: UHF9105) installed vertically as shown in Fig.3. A small size dipole antenna (probe) which is 40 mm length set with a balun (Murata Manufacturing: Chip multilayer hybrid balun) for mobile phone is used to detect the signal. The probe is connected to a coaxial cable from the top of phantom and is located inside at a position of 20 mm from the front surface. A power amplifier (Agilent Technology: 8347A) with 0.1 W output is installed at the transmitter and a pre-amplifier (Advantest: R14601) with 25 dB gain at the receiver. In order to suppress the unwanted scattered waves from the wall surface, we measure the *SE* in an anechoic chamber. Polyester fiber with copper and nickel plating are used as the material for the shielding clothes (slanted region in Fig.3).

Table 1. Material parameters

Phantom		
ε_r	49	
μ_r	1	
σ	1.6	S/m
Shielding material		
ε_r	1	
μ_r	1	
σ	1.5×10^5	S/m
Thickness	0.12	mm

4. Results and Discussions

The *SE* is evaluated at the observation point set at ① (x=220 mm, y=20 mm, z=400 mm) in the phantom model coordinates system in Fig.3. For comparison, the *SE* at point ② (x=150 mm, y=20 mm, z=400 mm) is also discussed. Further, the *SE* is obtained by changing the distance d between phantom surface and the transmitting antenna. Here, the x and z values of the transmission point are the same as those of the observation point. The transmission point is moved only in the y-direction.

4.1 Evaluation of E-field *SE* Usually a transmitting antenna and a receiving antenna are arranged to have the identical polarization (in z direction in Fig.3) when measuring the *SE*. However, with an aperture, the *SE* obtained by vector intensity $|\boldsymbol{E}|$ differs from that by one component $|E_z|$ as shown in Fig.4. This suggests that the polarization of the EM wave incoming from the aperture is changed by diffraction. Therefore, it is necessary both for FDTD analysis and experiment to evaluate $|\boldsymbol{E}|$ for obtaining the *SE* of the shielding clothes with aperture. Thus we have evaluated the *SE* in terms of $|\boldsymbol{E}|$ in this paper. However, without aperture, the *SE* is the same for $|\boldsymbol{E}|$ and $|E_z|$ as shown in Fig.4. Although not indicated in this figure, the *SE* without

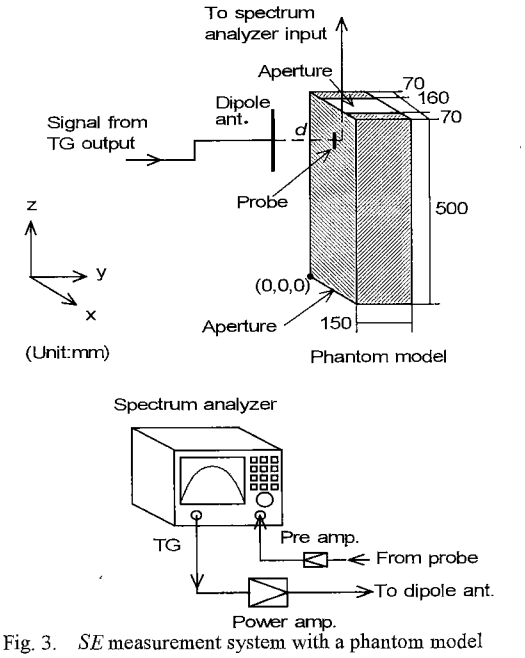

Fig. 3. *SE* measurement system with a phantom model

aperture has agreed with the theoretical result [13] of infinite plane shield.

4.2 Comparison with Experimental Result Fig.5 shows the comparison of the *SE* obtained by the FDTD analysis with that by the experiment, where the *SE* when the inside of the phantom is filled with air instead of saline is also plotted for comparison. It is indicated that the FDTD analytical result agrees with the experimental result within the error range of 3 dB, and this verifies the validity of the developed method. We can observe that as the distance *d* increases, the amount of diffracted wave from the top aperture also increase, causing the *SE* to decrease. In the case of air used as the inner medium of the phantom, since the amount of diffracted wave is less attenuated, the *SE* decreases. It can also be inferred that the *SE* improves at point ① than at ② because of the shielding material of the phantom shoulder region.

4.3 Shapes of Shielding Clothes The *SE* is compared among 4 types of shielding clothes at the observation point ① as shown in Fig.6. Type (a) is a base model. Type (b) and type (c) are assumed to be an apron and a pocket, respectively. For comparison with type (c), a shielding cloth of type (d) is calculated.

The result is shown in Fig.7 and indicates a difference of 10 dB between type (a) and type (b), since the amount of EM wave diffracting from the top and sides of shielding clothes increases. Further the *SE* shows slightly higher value in type (c) than in type (b). Because the observation point is located at the center of the shielding material in the case of type (c), the diffracting EM wave is mutually cancelled and then electric field intensity decrease, therefore the *SE* seems to increase. In the case of type (d), the observation point is also located at the center of the shielding material. However, in this case, the *SE* is worst among these shielding clothes types. Because material height of this type is shorter than antenna length, the amount of diffracted wave increases. As shown in Fig.8, when a location of the observation point is changed for type (c) and type (d) in the x-direction, the *SE* decreases greatly at the points without shielding cloth.

Next, Table 2 shows that the *SE* almost disappears for a shielding cloth of W:20×H:20 mm. We can observe that the *SE* tends to depend on material height rather than width in the case of a vertically transmitting antenna.

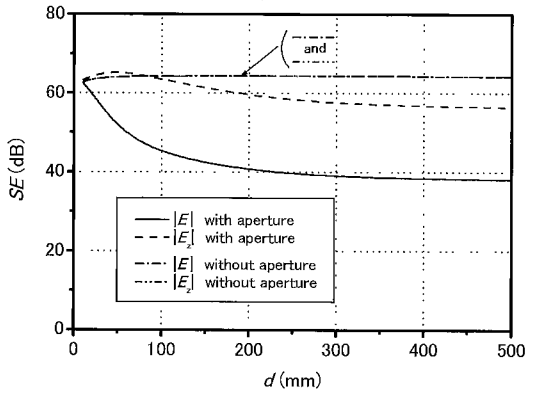

Fig. 4. *SE* calculation with $|\boldsymbol{E}|$ and $|E_z|$ at the observation point ①

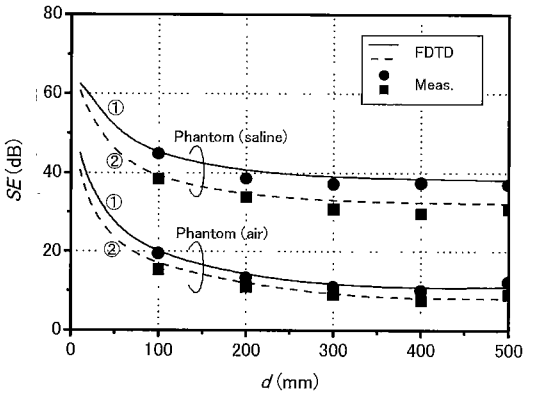

Fig. 5. FDTD analysis and experimental measurement of *SE* at the observation points ① and ②

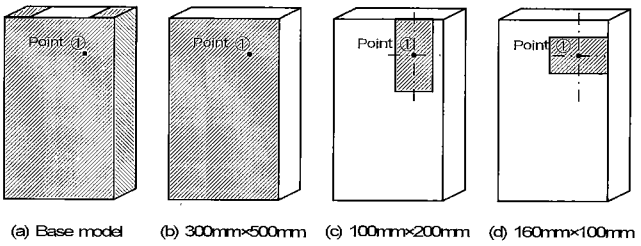

Fig. 6. Four types of shielding clothes

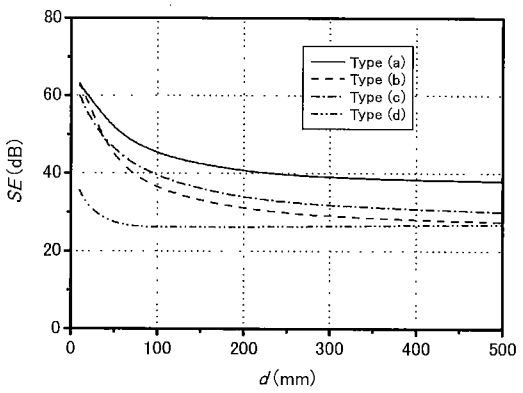

Fig. 7. *SE* dependence on the shapes of shielding clothes at the observation point ①

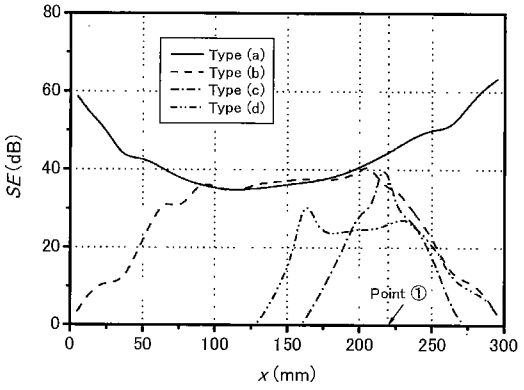

Fig. 8. *SE* dependence on the observation point. The observation point is moved toward x-direction. Transmitting antenna position is located at (220,-100,400) (*d*=100mm)

Table 2. *SE* dependence on the sizes of shielding cloth at the observation point ① (d=100mm)

W×H (mm)	*SE* (dB)	W×H (mm)	*SE* (dB)
100×200	38 6	50×100	20 3
160×100	26.1	100×50	11.0
100×160	38.7	50×50	7.6
100×100	26 1	20×20	0 5

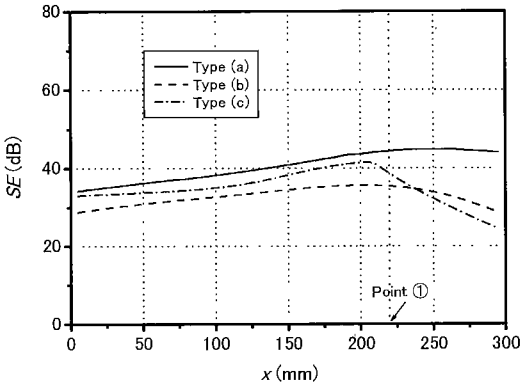

Fig. 9. *SE* dependence on the transmitting antenna position at the observation point ①. The transmitting antenna position is moved toward x-direction. (d=100mm)

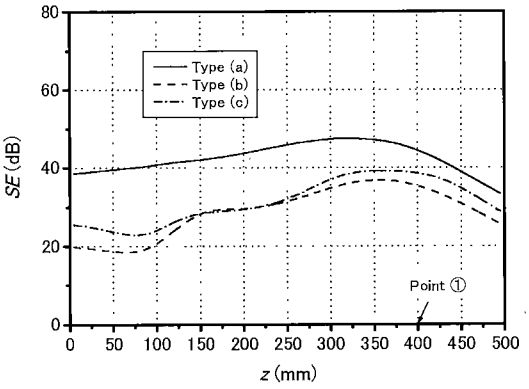

Fig. 10. *SE* dependence on the transmitting antenna position at the observation point ①. The transmitting antenna position is moved toward z-direction. (d=100mm)

4.4 Transmitting Antenna Position Dependence We investigate the effect of transmitting antenna position for the *SE*. Fig.9 and Fig.10 show the *SE* dependence on the x and z values of the transmitting antenna position. These figures show that the *SE* is higher in type (c) than in type (b) overall, as in Fig.7. Since EM wave diffracts from the side of the phantom, it is shown that the *SE* of type (a) which has shield material on a side region is large in Fig.9. When a transmitting antenna is located at the left side of the phantom (the right side of point ① in Fig.9), the *SE* shows higher value in type (b) than in type (c) because the amount of EM wave diffracted from the front and left side of the phantom increases.

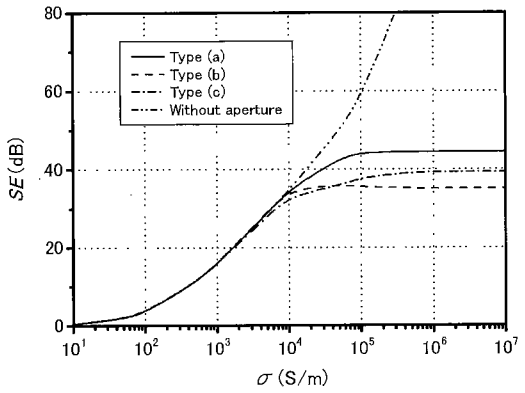

Fig. 11. Relationship between σ and *SE* at the observation point ① (d=100mm)

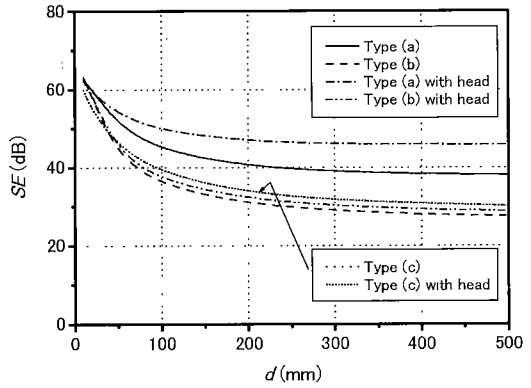

Fig. 12. Effect of human head on *SE* at the observation point ①

Similarly, since EM wave diffracts from the top of the phantom, it is shown that the shielding effectiveness of type (a) which has shield material in a shoulder region increases in Fig.10.

4.5 Conductivity of Shielding Clothes Fig.11 shows the *SE* when the conductivity σ of shielding clothes is varied. The *SE* first tends to increase by increasing σ. However, with an aperture (in type (a), type (b) and type (c)), there exists a point where the *SE* does not change even by increasing σ. This shows that the electric field intensity coming from the aperture becomes larger than the intensity of the EM wave transmitted through the shielding material. It is obvious that the effect is so remarkable for the larger aperture. However, as shown in paragraph 4.3, The *SE* shows higher value in type (c) than in type (b) by increasing σ. Therefore the *SE* would be hardly improved by increasing σ in the case of shielding clothes with apertures. From another viewpoint, the materials with too high conductivity are not necessary to effectively shield the EM wave.

4.6 Effect of Phantom Head Region We have studied the phantom model as a box model so far. In FDTD, we set up a head model (W:160×D:150×H:200 mm) at the top center of the phantom to observe the effect thereof. The result is given in Fig.12. Here, the electric parameters of the head region are the same as those of the torso region. The figure indicates that with the head region taken into consideration, the *SE* is improved except in type (c). In other words, the head region attenuates the amount of EM wave incoming through the top aperture,

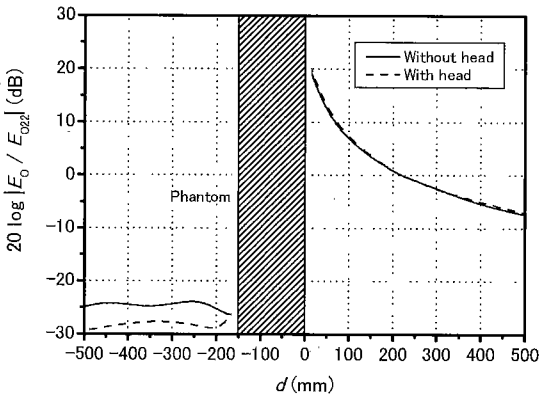

Fig. 13. Relationship between d and normalized electric intensity $|E_O/E_{O22}|$ at the observation point ① (without shielding clothes)

consequently reducing the electric field intensity at the observation point, and improving the *SE*. In the case of type (c), this figure shows that the head region does not affect the *SE*, since this cloth size is smaller.

4.7 Comparison with Guideline It is recommended in the guideline that the mobile phone should be used at a distance 22 cm or more from the cardiac pacemaker user. We calculate the electric field intensity E_o (observation point ① at an arbitrary d) normalized by the electric field intensity E_{o22} (observation point ① at d=22 cm from the transmitting antenna without the shielding clothes). The result is shown in Fig.13. In the figure, the negative d indicates that the transmitting antenna is located at the backside of the phantom. The positive value in vertical axis in the figure is equivalent to the *SE* needed for safety. It is found from the figure that the *SE* should be about 20 dB or more at the distance d=22 cm or less. Therefore, wearing the above shielding clothes would ensure safety even if the mobile phone is used closer than 22 cm. It also satisfies the guideline standards without suppressing the EM wave by shielding material when the transmitting antenna is located at the backside of the phantom. And the electric field intensity is smaller with the head region than without the head region in the case of the transmitting antenna located at the backside of the phantom, since amount of diffracted wave is attenuated by the head region.

5. Conclusion

We introduced the transmission coefficient when an EM wave is incident into a multi-layered material with an arbitrary direction, into the FDTD method to realize the 3-D numerical analysis of the EM wave transmission into the thin plate shielding material, which has conventionally been considered difficult. In the analysis, we used a phantom model as a dummy cardiac pacemaker user to study the EM *SE* by shielding clothes. In order to verify the validity of the developed FDTD algorithm, we analyzed the *SE* of shielding clothes, assuming that the clothes is made up of a single-layered shielding material. The analytical result is in good agreement with the experimental result, which demonstrates the validity of the developed FDTD method. We considered the effect of the aperture on the clothes and found that the amount of EM wave from the aperture becomes larger than the amount of EM wave transmitted through the shielding clothes. Thus, the aperture was found to be the major factor causing the *SE* to decrease. This suggests that in developing the shielding clothes, they should be designed to reduce the diffracted waves from the apertures. On the other hand, although a multi-layered material and a material with high electric conductivity can improve the *SE*, they are not necessary for the cases when the diffraction of EM wave from the aperture is dominant. The report presented here is limited to the specific phantom model, so that actually we have to investigate further models.

The FDTD analysis method developed here is applicable to the design of enclosure of electronic equipment in addition to the electromagnetic shielding analysis of shielding clothes for preventing the malfunction of cardiac pacemaker. Also, this method can be easily applicable to the multi-layered shielding material made of plastic material with metal plating, or double shielding material with an air gap [7].

Acknowledgement

This study was performed through Special Coordination Funds for Promoting Science and Technology (Leading Research Utilizing Potential of Regional Science and Technology) of the Ministry of Education, Culture, Sports, Science and Technology of the Japanese Government.

(Manuscript received April 26,2002, revised January 24,2003)

References

(1) T Toyoshima, M Tsumura, T.Nojima, and Y.Tarusawa : "Electromagnetic Interference of Implantable Cardiac Pacemakers by Portable Telephones", *Cardiac Pacing*, Vol.12, No 5, pp.488-497 (1996)

(2) M W Chevalier, R.J Luebbers, and V.P.Cable : "FDTD Local Grid with Material Traverse", *IEEE Trans. Antennas Propagat*, Vol.45, No.3, pp.411-421 (1997)

(3) S.Van den Berghe, F.Olyslager, and D.D.Zutter : "Accurate Modeling of Thin Conducting Layers in FDTD", *IEEE Microwave Guided Wave Lett*, Vol 8, No.2, pp 75-77 (1998)

(4) C J Railton and J.P.McGeehan : "An Analysis of Microstrip with Rectangular and Trapezoidal Conductor Cross Sections", *IEEE Trans. Microwave Theory Tech.*, Vol 38, No.8, pp.1017-1022 (1990)

(5) H.Ebara and O.Hashimoto "A Study on Modeling of Resistive-film using Approximate Equation of the Resistive-film for FDTD Analysis", *Trans. IEICE*, Vol.83-B, No.5, pp.748-751 (2000-5)

(6) T.Fukasawa, H Ohmine, I.Chiba, and Y.Sunahara: "Simulation of Transmission Waves through Multi Layered Thin Conducting Sheets by FDTD Method", *Trans. IEICE*, Vol.83-B, No.5, pp.711-719 (2000-5)

(7) Y.Yoshimura, I Nagano, S Yagitani, and S.Shinmura : "FDTD Analysis of Electromagnetic Shielding Effectiveness of Obliquely Incident Waves", *T. IEE Japan*, Vol.121-A, No.10, pp.964-965 (2001-10)

(8) S Nishizawa, O Hashimoto, and T.Ooi . "A study of Simplified E-Field Measurement inside the Dry Phantom Model", Tech. Rep. IEICE, EMCJ97-107, pp 55-61 (1998)

(9) J.Wang, O Fujiwara, and T.Nojima : "A Model for Predicting Electromagnetic Interference of Implanted Cardiac Pacemakers by Mobile Telephones", *IEEE Trans. Microwave Theory Tech.*, Vol.48, No.11, pp 2121-2125 (2000)

(10) S.Nishizawa and O.Hashimoto : "Near Field Shielding Effect for Oval Human Model using High Loss Magnetic and Dielectric Materials", Tech. Rep IEICE, EMCJ99-14, pp.41-46 (1999)

(11) S Kurokawa, T Sato, K.Hori, and K Ishihara : "Effect of Various Shielding on Mobile Phone Field Intensity in Human Body", Proc. 1999 Commun. Soc. Conf IEICE, B-4-27 (1999)

(12) J.Wang, T Ohshima, and O.Fujiwara : "Effectiveness Evaluation of Shielding Material in Reducing Electromagnetic Interference of Cardiac Pacemaker Induced by Portable Infomation Terminals", *Trans. IEICE*, Vol.84-B, No.10, pp.1829-1833 (2001-10)

(13) Y.Yoshimura, I.Nagano, S.Yagitani, T.Ueno, and T.Ooura . "Shielding and Absorption by a Multilayered Material for Electromagnetic Waves with Oblique Incidence", Tech. Rep. IEICE, EMCJ2001-5, pp.25-30 (2001)

(14) Y.Yoshimura, T.Ueno, I.Nagano, S.Yagitani, and S.Shinmura : "FDTD Analysis of Electromagnetic Wave Reduction Effect by Shielding Clothes", 2002 National Convention Record, IEE Japan [1], p.267 (2002)

(15) I.Nagano, Y Yoshimura, S.Yagitani, H.Yokomoto, T.Tosaka, and T.Nakayabu . "Estimation of Electric Parameters of Thin Electromagnetic Shielding Materials", *T. IEE Japan*, Vol.123-A, No 2, pp.192-199 (2003-2)

(16) T.Yamashita "Study of a small antenna in the vicinity of human body", Master's Thesis, Kanazawa University (2000)

(17) T Ueno, Y.Yoshimura, I Nagano, and S.Yagitani. "FDTD Analysis of Electromagnetic Shielding Effectiveness of Shielding Clothes on a Human Model", Tech. Rep. IEICE, AP2001-76, pp.21-25 (2001)

(18) T Uno : Finite Difference Time Domain Method for Electromagnetic Field and Antenna Analyses, pp.151-157, Corona Publishing Co., Ltd. (1998)

Yoshiyuki Yoshimura (Student Member) He received the B.E. and the M.E. degrees in Mechanical Systems Engineering from Nagaoka University of Technology, in 1988 and 1990, respectively. Since 1990, he has been with Industrial Research Institute of Ishikawa, Product and Technology Department, where he is now a Researcher. He is engaged in research electromagnetic interference/compatibility (EMI/EMC) problems. He is now studying toward Ph.D. degree in Kanazawa University. He is a member of the Institute of Electronics, Information and Communication Engineers (IEICE) of Japan.

Isamu Nagano (Member) He received the B.E, and M.E. degrees from Kanazawa University in 1968 and 1970, respectively and Dr.E. degree in Electrical Engineering from Kyoto University in 1980. Since 1970, he has been with Kanazawa University, Department of Information and Systems Engineering, where he is now a Professor of radio wave science and engineering. From 1982 to 1983, he was an NRC Resident Research Associate at NASA Jet Propulsion Laboratory. His research fields are the theoretical and experimental studies of electromagnetic wave propagation in geospace using rockets and satellites, and of EMI/EMC problelms. He was awarded TanakaDate Prize in 1987, NASA Group Achievement Award in 1998, and *Hokkoku Bunka* Prize in 2000. He is a member of the IEICE of Japan, the Society of Geomagnetism and Earth, Planetary and Space Sciences (SGEPSS) of Japan, and a member of American Geophysical Union (AGU).

Satoshi Yagitani (Non-Member) He received the B.E., the M.E., and the Dr.E. degrees in Electrical and Computer Engineering from Kanazawa University, Kanazawa, Japan, in 1988, 1990, and 1993, respectively. Since 1993, he has been with Kanazawa University, Department of Information and Systems Engineering, where he is now an Associate Professor of radio wave science and engineering. From 1997 to 1998, he was a visiting researcher at the University of Minnesota. His research interests are plasma wave propagation in geospace, the analysis of wave field data obtained by satellites, and EMI/EMC problems. He was awarded *Sangaku Renkei Suishin Ishikawa Shourei* Prize in 2001. He is a member of the IEICE of Japan, the SGEPSS of Japan, and a member of AGU.

Tomohiko Ueno (Non-Member) He received the B.E. and the M.E. degrees in Information and Systems Engineering from Kanazawa University, in 2000 and 2002, respectively. Since 2002, he has been with PFU Limited.

Toshio Nakayabu (Non-Member) He received the B.E. and the M.E. degrees in Mechanical Engineering from Kanazawa University, in 1971 and 1974, respectively. Since 1974, he has been with Industrial Research Institute of Ishikawa, Product and Technology Department, where he is now a Manager. His research interest is measurement by laser interferometry for machine tool. He is a member of Japan Society Mechanical Engineers (JSME) and a member of Japan Society for Precision Engineering (JSPE).